Experimental Supplement to the first HyDRA blind challenge

Version 2 (March 1, 2023), including remeasurements after the theory submissions

Taija L. Fischer[a], Margarethe Bödecker[a], Sophie M. Schweer[a], Jennifer Dupont[b], Valéria Lepère[b], Anne Zehnacker-Rentien[b], Martin A. Suhm[a]*

[a] *Institut für Physikalische Chemie, Universität Göttingen, Tammannstr. 6, 37077 Göttingen, Germany;* [b] *Institut des Sciences Moléculaires d'Orsay, Université Paris-Saclay, CNRS, 91405, Orsay, France*

Abstract

The experimental spectroscopic results on the 10 test monohydrates of the first HyDRA blind challenge are summarized. These were kept confidential until the final deadline for submission and editing of theoretical predictions and pre-published under https://doi.org/10.25625/FLGZYE without any prior knowledge of the computed results of theory submissions. The present version also includes a re-investigation of a training set member, the monohydrate of aniline.

*please send all correspondence to M. A. Suhm (msuhm@gwdg.de)

1 Introduction

This document summarizes the experimental results on the test set of the HyDRA blind challenge[1,2]. For the 10 systems in the test set, selected experimental spectra are shown and the assigned hydrogen-bonded water OH-stretching bands OH_b are labeled. The most important observations and transition wavenumbers (in cm^{-1}, in some cases also adding estimated full widths at half maximum FWHM of the observed bands) are briefly summarized, to be compared to theoretical submissions. Section 4 contains the spectra obtained in a reinvestigation of the aniline monohydrate a member of the training set.

2 Translation and summary table

Table 1 provides a translation between the compounds in the test set (see also Figure 1), their acronyms used in the previous preprint[1] and follow-up publication[2], and the BC## code which was used internally during the blind phase of the challenge to help protect the experimental data. This code is kept here for easier reference to raw data.

Table 1: Test set of 10 acceptor molecules – abbreviations, codes used during the blind challenge to protect the data (BC##) and expected minimum number of OH stretching signals in the most stable monohydrate n(OH), among which the hydrogen-bonded water OH_b wavenumber (considering the experimental water monomer fundamental at $3657\,cm^{-1}$) should be predicted. The actual value $\tilde{\nu}_{exp}(OH_b)/cm^{-1}$ determined in this work is listed in the last column (see text for error bars and entries in curly brackets).

acceptor molecule	abbreviation	BC code	n(OH)	$\tilde{\nu}_{exp}(OH_b)/cm^{-1}$
Cyclooctanone[3,4]	CON	BC22	2	3503(1)
1,3-Dimethyl-2-imidazolidinone[5,6]	DMI	BC27	2	3492(2)
Formaldehyde[7,8]	FAH	BC02	2	3591(2)
Methyl lactate[9,10]	MLA	BC30	3	3524(2) {3474(3)}
1-Phenylcyclohexane-cis-1,2-diol[11]	PCD	BC36	4	$3597(+4,-2)$
Pyridine[12,13]	PYR	BC16	2	3454(1)
Tetrahydrofuran[14,15]	THF	BC20	2	3491(1)
Tetrahydrothiophene[16]	THT	BC29	2	3507(1)
2,2,2-Trifluoroacetophenone[17]	TPH	BC18	2	3611(1)
2,2,2-Trifluoroethan-1-ol[18,19]	TFE	BC38	3	3649(1)

The table also summarizes the core experimental result for each system, obtained and presented here for the first time. Uncertainties ($\pm$ the number given in parentheses) are chosen according to the spectral resolution, including wavenumber calibration uncertainty, and the spectral width and potential congestion. Where the uncertainties are believed to be asymmetric due to a spectral feature, they are provided explicitly ($+-$). Where the OH_b character is evidently

shared among two bands, the minor contributor is listed in curly brackets. For n(OH)>2 (i.e. alcohols with their own OH stretching vibration), we recommend that the theory groups report all OH stretching fundamentals, because there may be mode mixing between the hydrogen-bonded alcoholic and water OH bonds. Alternatively, we recommend to report the mode which shows the strongest downshift when $H_2{}^{16}O$ is replaced by $H_2{}^{18}O$, because it carries the strongest water stretching character.

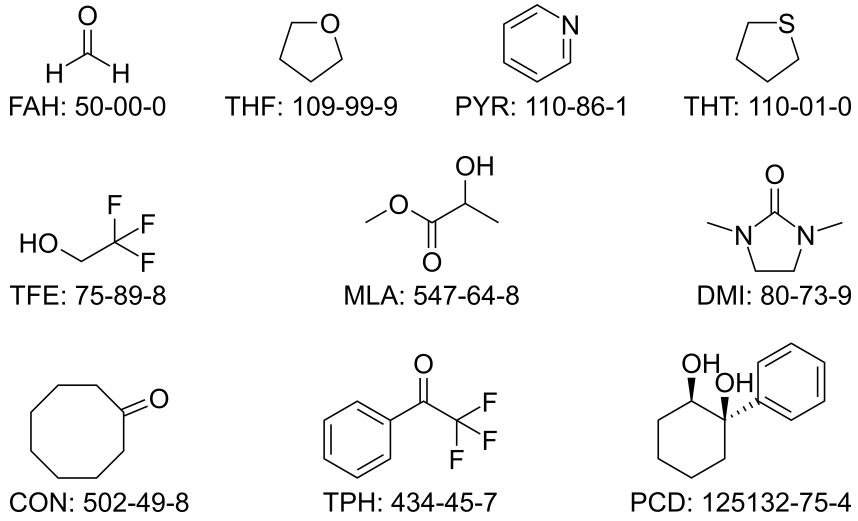

Figure 1: The structural formulas, abbreviations, and CAS registry numbers of the 10 systems selected for the HyDRA test set.

3 Test set

Among the ten systems in the test set, one was characterized by ionization-detected UV/IR double resonance pinhole jet spectroscopy[20], two by Raman slit jet spectroscopy[21] and eight by FTIR slit jet spectroscopy[22]. Where partial pressures for the components in the expanding gas jet are provided, they represent rough estimates based on gas pre-mixing or flow metrology in combination with saturation vapor pressures, sometimes corrected for wall desorption by comparing monomer signals. They are only meant to provide some guidance on the scaling behaviour of the monohydrate complex signals.

3.1 BC02+H_2O

BC02 was obtained as the chemically bound cyclic trimer from Alfa Aesar (97%, Lot#10165222), degassed and decomposed into monomeric BC02 by heating the solid up to a desired partial pressure. Partial pressures are therefore particularly approximate for this compound. Different amounts of H_2O (explicitly added + desorbed from the walls) or D_2O (99.85%, Abcr, AB 403423, slowly H/D-exchanging during the measurement, therefore only a selection of early scans from

three fresh fillings was used, a D in the table marks D_2O partial pressures) were added to the expansion gas (750 hPa He, a Ne is added if neon is used instead). For the spectra # gas pulses were co-added.

identifier	# pulses	p(BC02) hPa	$p(H_2O)$ hPa	p(He) hPa	note
20211126-abcd	800	0.8	0.4	750	see figure 2, upper panel, black
20211125-abcd	800	0.3	0.4	750	see figure 2, upper panel, blue
Gottschalk et al.[22] (Ne)	2200	0.0	0.5	750 Ne	see figure 2, upper panel, grey
20220119-ad+0120-abde	400	0.8	0.8D	750	see figure 2, lower panel, orange
Gottschalk et al.[22] (Ne)	1950	0.0	0.6D	750 Ne	see figure 2, lower panel, grey

The OH_b band of the BC02 monohydrate is located at 3591 cm^{-1} with a FWHM of about 6 cm^{-1} and a slight indication of rovibrational structure in the spectrum with the stronger signal even at the low spectral resolution employed. For such a light complex, K-rotational structure may be expected, but the available signal-to-noise ratio currently does not give access to this rotational structure. It cannot be excluded that the observed band involves K-rotational excitation. The OD_b band of the fully deuterated monohydrate of (presumably undeuterated) BC02 is located at 2629 cm^{-1} with a FWHM of about 5 cm^{-1}. It cannot be excluded that the H atoms of BC02 are partially deuterated as well in the expansion and recycling process.

The vacuum-isolated band position may be compared to previous matrix isolation measurements[7,23], which are systematically lower in wavenumber and split by the matrix interaction (3580, 3585 cm^{-1} in neon and argon, 3573, 3578 cm^{-1} in a nitrogen matrix).

Exploratory harmonic quantum chemical calculations on B3LYP-D3(BJ)/def2-TZVP level predict only one populated 1:1 complex isomer and thus one signal for the BC02+H_2O complex, consistent with the observations (see Fig. 2) and also with previous theoretical[24–26] and rotational spectroscopy[8] evidence.

Conclusion: One dominant conformation of the monohydrate with OH_b signal at 3591 cm^{-1} and with OD_b signal at 2629 cm^{-1}, no need to invoke a resonance or second isomer at the present S/N ratio. Raman detection may add further evidence for the assignment of the observed spectral features.

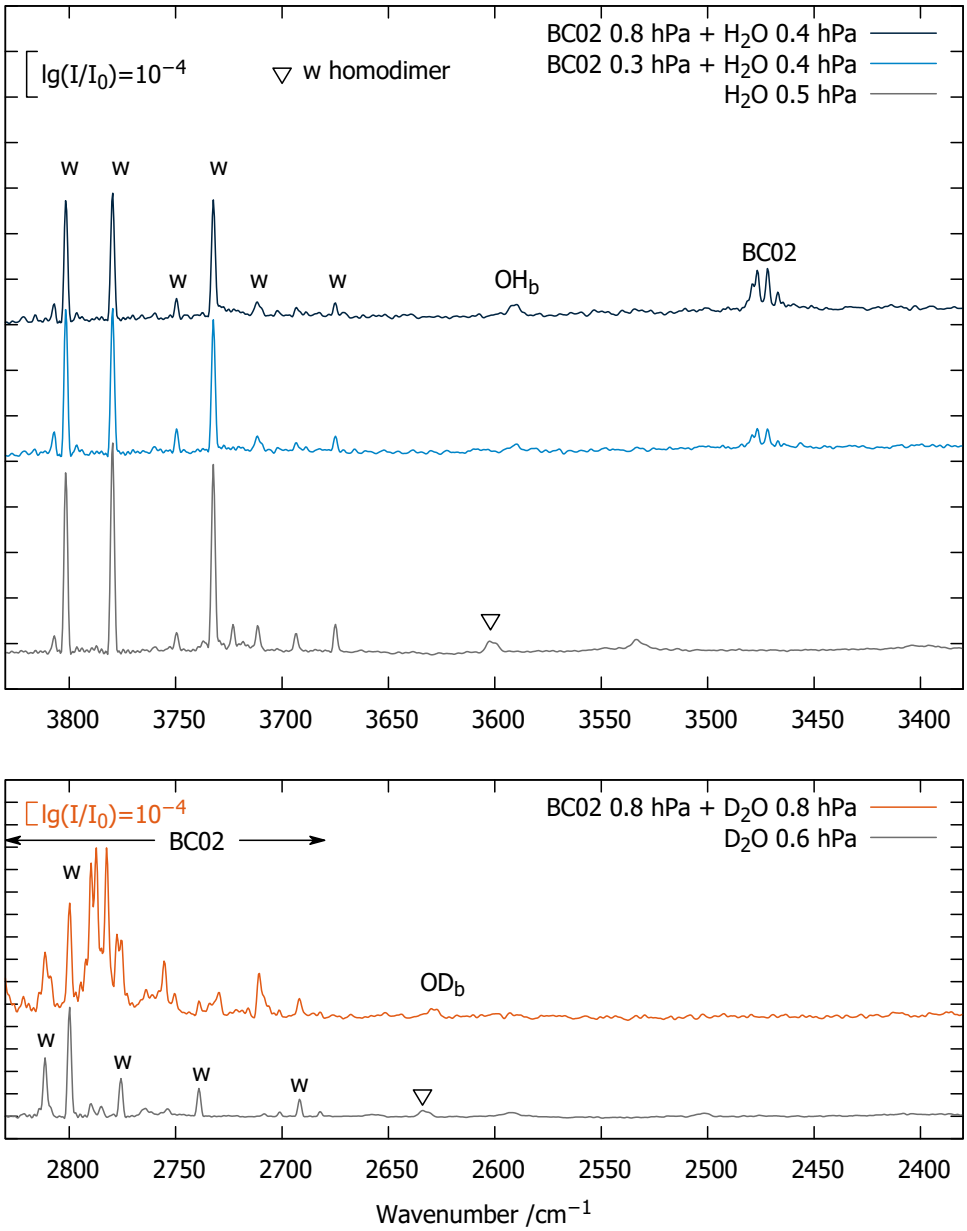

Figure 2: Jet cooled FTIR spectra of BC02 with H_2O (upper) and D_2O (lower panel). The heterodimer bands of donor water are labeled as OH_b (scaling more or less linearly with the water (w) concentration) and OD_b, respectively.

3.2 BC16+H_2O

BC16 was obtained from Sigma Aldrich (>99.9%, Lot#SHBL8071), degassed and measured at different partial pressures with different amounts of H_2O (explicitly added + desorbed from the walls) or D_2O (slowly H/D-exchanging, therefore only a selection of early scans from three fresh fillings was used, a D in the table marks D_2O partial pressures) in 750 hPa He, co-adding # gas pulses.

identifier	# pulses	p(BC16) hPa	p(H_2O) hPa	p(He) hPa	note
20210503-abcdefg	700	0.2	0.1	750	see figure 3, dark blue
20211013-abcde	800	0.2	0.3	750	see figure 3, light blue
20210511-abcdefg	800	0.3	0.3	750	not shown, similar to light blue
20210512-abgh+0510-ef	300	0.3	0.3D	750	see figure 3, orange

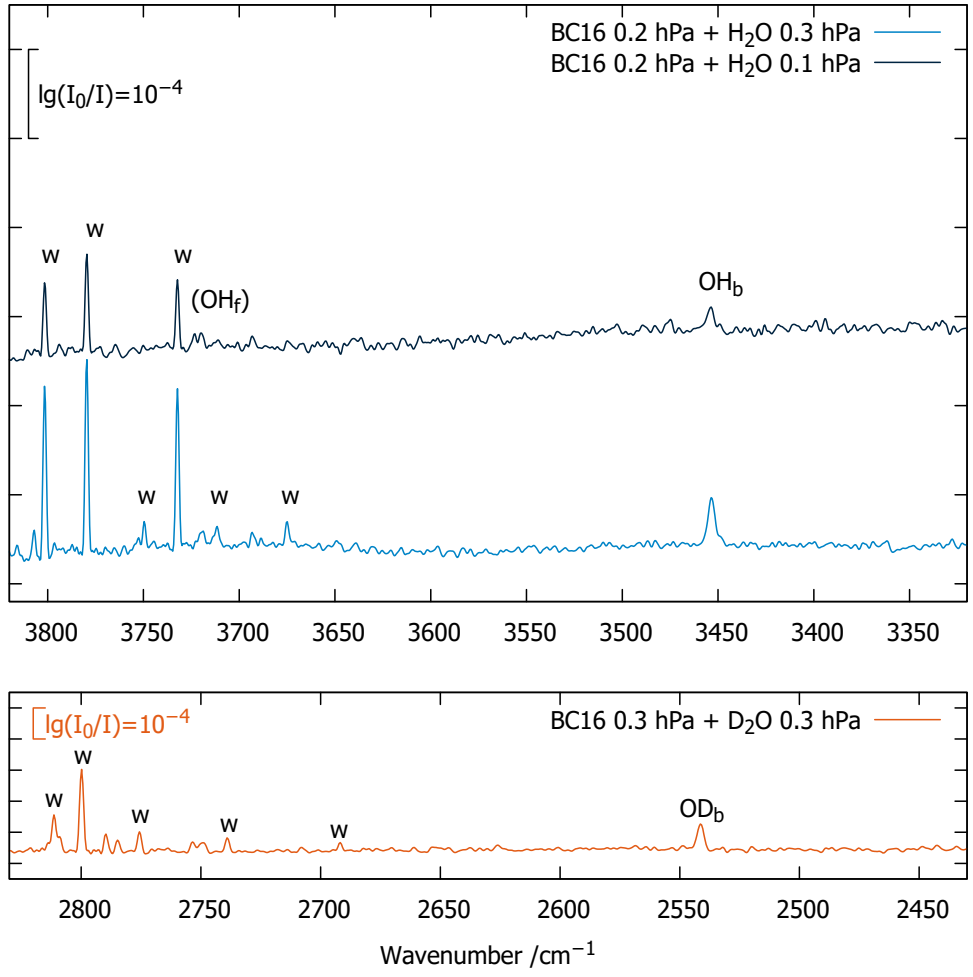

Figure 3: Jet cooled FTIR spectra of BC16 with H_2O (upper) and D_2O (lower panel). The heterodimer bands of donor water are labeled as OH_b (scaling more or less linearly with the water (w) concentration) and OD_b, respectively. The signal marked (OH_f) cannot be located reliably.

The OH_b band of the monohydrate is located at 3454 cm^{-1} with a FWHM of about 4 cm^{-1}. The OD_b band of the fully deuterated monohydrate is located at 2541 cm^{-1} with a FWHM of about 3 cm^{-1}. A side effect of the partial isotope exchange when introducing D_2O is the identification of the OH_b and OD_b bands of HDO coordinating at BC16 with its different hydrogen isotopes, near 3464 and 2549 cm^{-1}.

The room temperature gas phase value for the hydrogen-bonded OH stretching mode in PYR monohydrate[27] is 3480 cm^{-1}, significantly higher than the cold jet value reported here. While ultracold helium droplets should exhibit much smaller, but still significant[28,29] environmental shifts than a room temperature gas phase measurement, a corresponding recent study[12] does not address the relevant spectral range and isotope composition. The value obtained in Ar matrices[30] is much lower (3400 cm^{-1}), underscoring the need for cold gas phase spectroscopy data. A very recent IR-VUV study[31] was unable to identify the neutral monohydrate due to instability of the cationic counterpart.

Exploratory harmonic quantum chemical calculations on B3LYP-D3(BJ)/def2-TZVP level predict only one populated 1:1 complex isomer and thus one signal for the BC16+H_2O complex, consistent with the observations (see Fig. 3). The large amplitude tunneling dynamics of this complex[13] does not affect the appearance of the low resolution IR spectrum.

Conclusion: One dominant conformation of the monohydrate with OH_b signal at 3454 cm^{-1} and with OD_b signal at 2541 cm^{-1}, no need to invoke a resonance or second isomer at the present S/N ratio.

3.3 BC18+H_2O

BC18 was obtained from Sigma Aldrich (>99%, Lot#BCCD3757), degassed and measured at a partial pressure of 0.2 hPa with different amounts of H_2O (explicitly added + desorbed from the walls) in 750 hPa He, co-adding # gas pulses. The sample with lower H_2O concentration is slightly affected by desorbing impurities from a preceding measurement of BC20 with D_2O, but these do not compromise the relevant spectral range.

identifier	# pulses	p(BC18) hPa	p(H_2O) hPa	p(He) hPa	note
20210602-abcdefg	800	0.2	0.1	750	see figure 4, blue
20210603-abcdef	700	0.2	0.2	750	see figure 4, dark blue

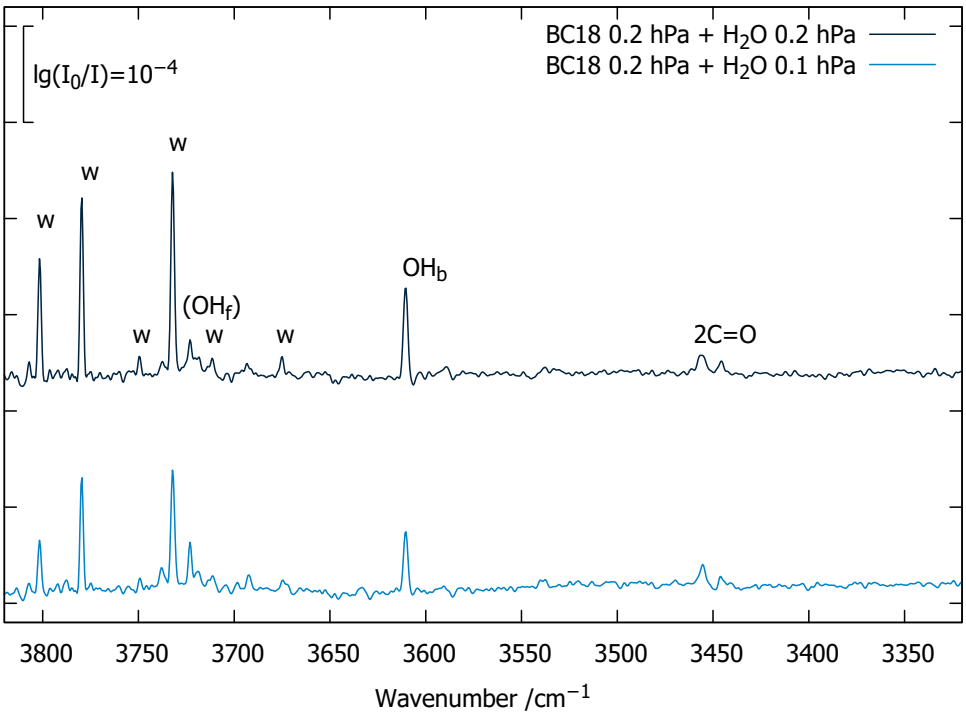

Figure 4: Jet cooled FTIR spectra of BC18 with more (upper) and less (lower trace) H_2O. The signal marked as OH_b scales with the water (w) concentration. The signal marked (OH_f) cannot be located reliably. The doublet signal marked 2C=O is dominated by the C=O overtone of the ketone.

The OH_b band of the monohydrate is located at 3611 cm^{-1} with a FWHM of about 3 cm^{-1}.

Exploratory harmonic quantum chemical calculations on B3LYP-D3(BJ)/def2-TZVP level predict only one populated 1:1 complex isomer and thus one signal for the BC18+H_2O complex, consistent with the observations (see Fig. 4) and its detailed structural characterization[17].

Conclusion: One dominant conformation of the monohydrate with OH_b signal at $3611\,cm^{-1}$, no need to invoke a resonance or second isomer at the present S/N ratio.

3.4 BC20+H_2O

BC20 was obtained from Sigma Aldrich (>99.9%, Lot#SSTBK0557), degassed and measured at different partial pressures with different amounts of H_2O (explicitly added + desorbed from the walls) or D_2O (slowly H/D-exchanging, a D in the table marks D_2O partial pressures) in 750 hPa He, co-adding # gas pulses.

identifier	# pulses	p(BC20) hPa	p(H_2O) hPa	p(He) hPa	note
20211012-abcde2	800	0.2	0.2	750	see figure 5, dark blue
20210831-abcdf	900	0.1	0.1	750	see figure 5, blue
20210901-abcde	800	0.1	0.25	750	see figure 5, light blue
20210526-abgh+0527-abgh	400	0.2	0.2D	750	see figure 5, orange

The OH_b band of the monohydrate is located at 3491 cm^{-1} with a FWHM of about 4 cm^{-1}. The OD_b band of the fully deuterated monohydrate is located at 2568 cm^{-1} with a FWHM of about 4 cm^{-1}. A side effect of the partial isotope exchange when introducing D_2O is the identification of the OH_b and OD_b bands of HDO coordinating at BC20 with its different hydrogen isotopes, near 3503 and 2579 cm^{-1}.

The vacuum-isolated band position of the monohydrate may be compared to previous CCl_4 solution[32] results at 268 K, which show a broad (about 80 cm^{-1} FWHM) hydrogen-bonded OH stretching fundamental near 3450 cm^{-1} at high dilution. Pseudorotational dynamics of the monomer[14,33] does not appear to complicate the monohydrate vibrational spectrum.

Exploratory harmonic quantum chemical calculations on B3LYP-D3(BJ)/def2-TZVP level predict only one populated 1:1 complex isomer and thus one signal for the BC20+H_2O complex, consistent with the observations upon BC20 and H_2O variation (see Fig. 5) and previous computational evidence[15].

Conclusion: One dominant conformation of the monohydrate with OH_b signal at 3491 cm^{-1} and with OD_b signal at 2568 cm^{-1}, no need to invoke a resonance or second isomer at the present S/N ratio.

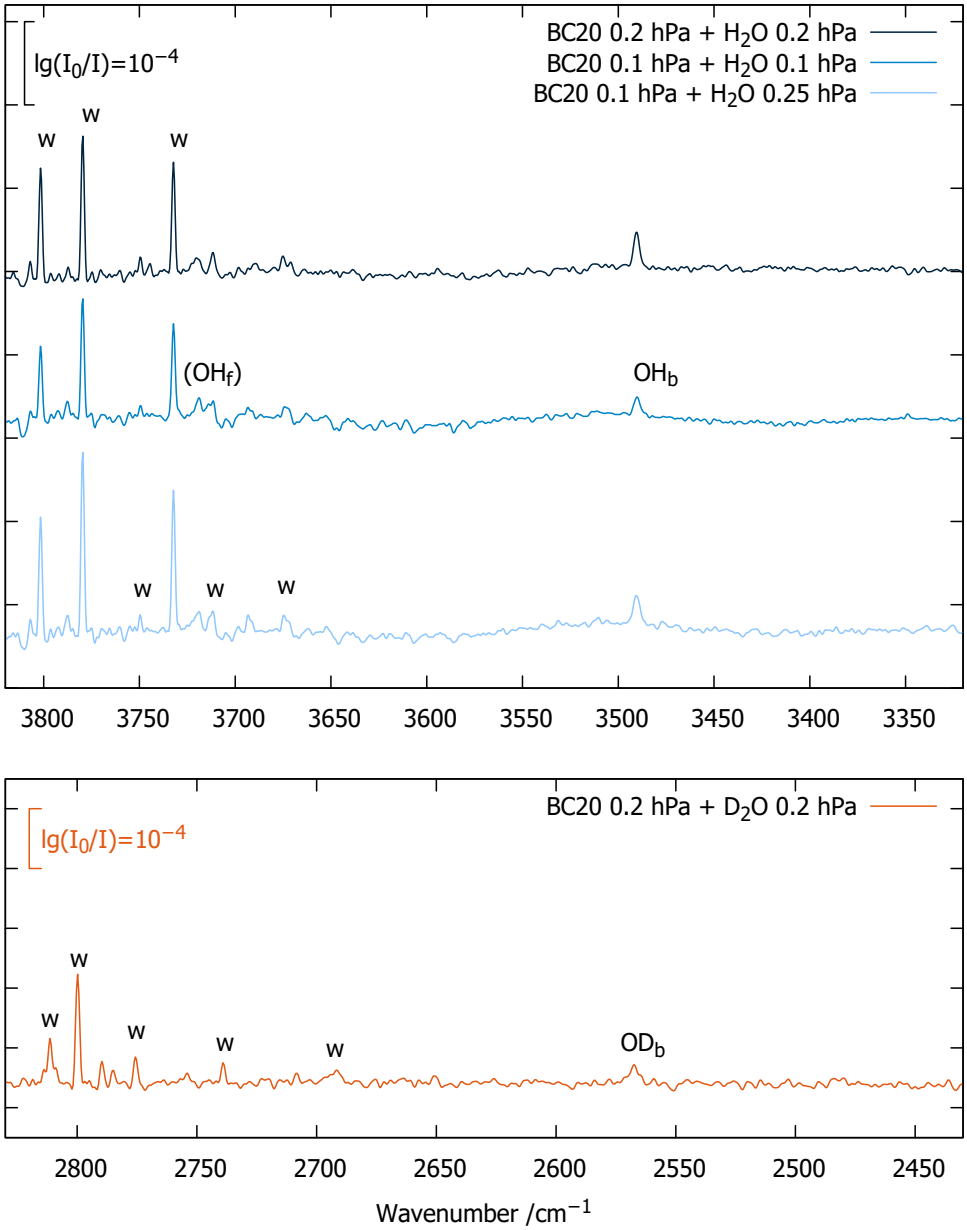

Figure 5: Jet cooled FTIR spectra of BC20 with H_2O (upper panel, in different ratios for the traces in blue shades) and D_2O (lower panel, orange). The heterodimer bands of donor water are labeled as OH_b (scaling more or less linearly with the water (w) and BC20 concentration) and OD_b, respectively. The signal marked (OH_f) cannot be located reliably.

3.5 BC22+H_2O

BC22 was obtained from Sigma Aldrich (98%, Lot#MKBN3780V), degassed and measured at different partial pressures with different amounts of H_2O (explicitly added + desorbed from the walls) or D_2O (slowly H/D-exchanging, a D in the table marks D_2O partial pressures) in the expansion gas (750 hPa He, a Ne is added if neon is used instead), co-adding # gas pulses.

identifier	# pulses	p(BC22) hPa	p(H_2O) hPa	p(He) hPa	note
20211015-abcd	700	0.1	0.1	750	see figure 6, dark blue
20211014-abcde	800	0.1	0.2	750	see figure 6, blue
20210430-abcde	500	0.1	0.1	375 Ne	see figure 6, light blue
20210426-a+0427-ag	150	0.2	0.2D	750	see figure 6, orange

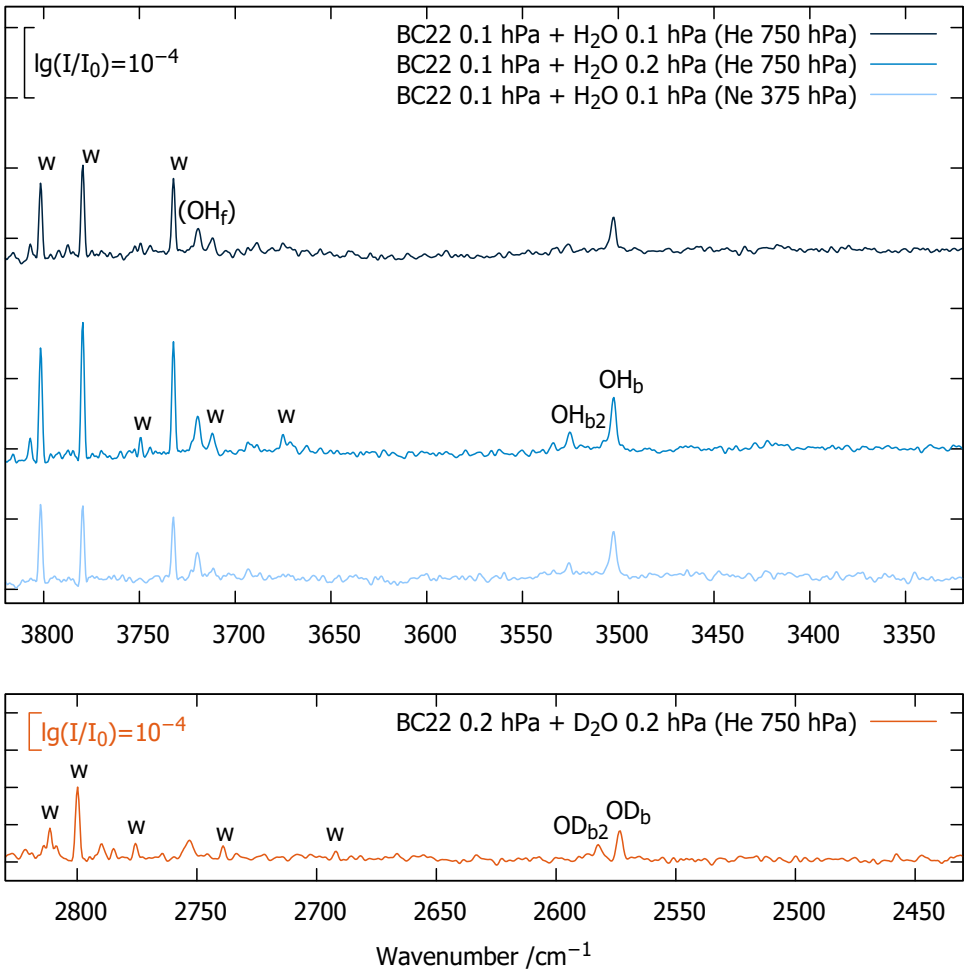

Figure 6: Jet cooled FTIR spectra of BC22 with water H_2O (upper) and D_2O (lower panel). Two significant signals (major signal O(H/D)$_b$, minor signal O(H/D)$_{b2}$, depending on expansion conditions) of complexes are observed independent on the isotopolog, supporting an isomer assignment instead of a resonance assignment.

The dominant OH_b band of the monohydrate is located at 3503 cm^{-1} with a FWHM of about

4 cm^{-1}. The OD_b band of the fully deuterated monohydrate is located at 2573 cm^{-1} with a FWHM of about 3 cm^{-1}. We suggest that these numbers should be compared to the most stable predicted 1:1 complex isomer, assuming no resonance situation in the absence of clear evidence thereof. If the metastable isomer (where the water probably coordinates the other C=O lone pair, see the microwave evidence[3]) is discussed, it should be tentatively compared to the experimental OH_{b2} band at 3525 cm^{-1} and the experimental OD_{b2} band at 2583 cm^{-1}. Notably, the 2583 cm^{-1} band is almost as intense as its isomer, possibly indicating a smaller energy difference between the two isomers for D_2O. The interpretation of the minor peaks as b2lib resonances[34] of the main isomer is unlikely due to the persistence of the pattern upon deuteration.

A side effect of the partial isotope exchange when introducing D_2O is the identification of the OH_b and OD_b bands of HDO coordinating at BC22 with its different hydrogen isotopes, near 3517 and 2587 cm^{-1} (FWHM 3 cm^{-1}). The 14 cm^{-1} blue shift is characteristic for the removal of the coupling between near-degenerate water stretching modes in HDO. For the metastable isomer, the situation is more complex, not only due to its reduced population. The OH_{b2} and OD_{b2} bands of HDO coordinating at BC22 are observed at 3534 and 2599 cm^{-1}, i.e. 9 and 16 cm^{-1} higher than the symmetric water isotopologs. Now, the OH stretching band for HDO also gains intensity relative to the H_2O case. It will be interesting to come back to these intensity anomalies in the light of anharmonic calculations. They may point at isotope-dependent isomerization energies or anharmonic resonances.

A complicating aspect which was recently discussed based on microwave evidence[3] is the possibility of geminal diol formation due to the chemical reaction of the ketone with the complexing water. Such a diol (uncoordinated or further hydrated) would show a different IR spectrum. The observation that the signals attributable to OH_f are somewhat more intense than in comparable systems may be related to such diol impurities, but this appears rather unlikely.

Exploratory harmonic quantum chemical calculations on B3LYP-D3(BJ)/def2-TZVP level predict two populated 1:1 complex isomers and thus two signal for the BC22+H_2O complex, consistent with the observations upon BC22 and H_2O variation (see Fig. 6). While the monomer can be safely assumed to be monoconformational at low temperature[3], the presence of two monohydrate isomers is expected based on structural spectroscopy[3].

Conclusion: The global minimum conformation of the BC22 monohydrate has an OH_b signal at 3503 cm^{-1} and an OD_b signal at 2573 cm^{-1}, any resonance affecting these transitions is difficult to quantify due to the potentially overlapping metastable monohydrate isomer.

3.6 BC27+H_2O

BC27 was obtained from Sigma Aldrich (reagent grade, Lot#STBK1255), degassed and measured at different partial pressures with different amounts of H_2O (explicitly added + desorbed from the walls) in 750 hPa He, co-adding # gas pulses.

identifier	# pulses	p(BC27) hPa	p(H_2O) hPa	p(He) hPa	note
20210625-adef	500	0.1	<0.1	750	see figure 7, dark blue
20210812-abcdefg	800	0.1	0.1	750	see figure 7, blue

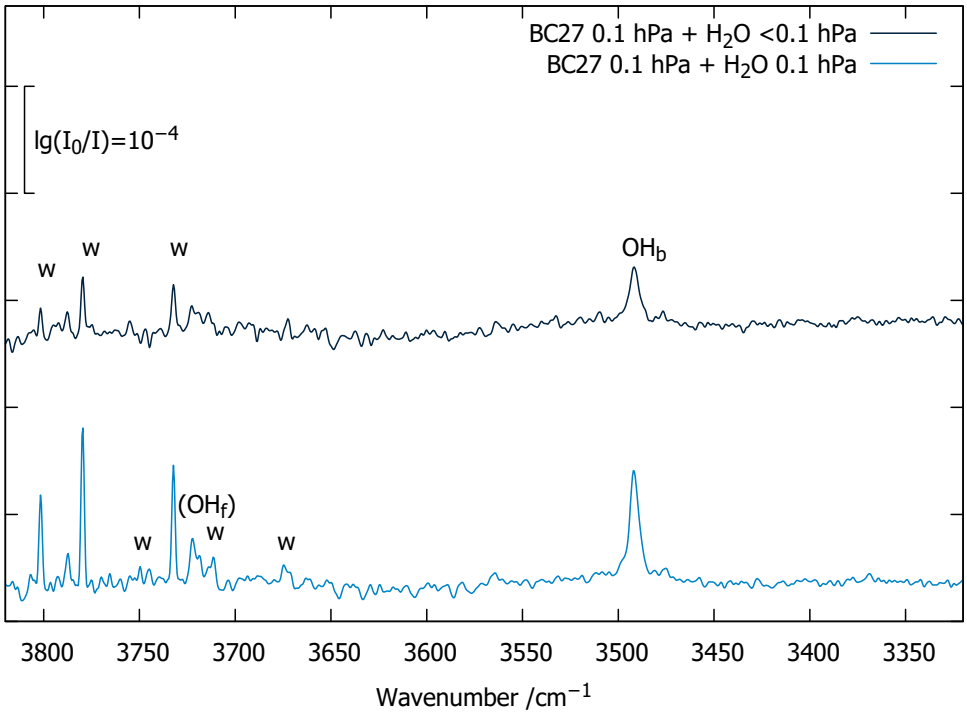

Figure 7: Jet cooled FTIR spectra of BC27 with H_2O. The signal marked with OH_b scales with the water and BC27 concentration like a 1:1 complex.

The measurements show only one signal for the heterodimer of BC27+H_2O at 3492 cm^{-1} with a FWHM of about 6 cm^{-1} and the assignment is straightforward (see Fig. 7). The vacuum-isolated band position may be compared to the broad absorption maxima due to the monohydrate in solution[5] (3431 cm^{-1} in 1,2-dichloroethane and 3460 cm^{-1} in CCl_4)

Exploratory quantum chemical calculations on B3LYP-D3(BJ)/def2-TZVP level predict only one stable heterodimer structure, consistent with the observations.

Conclusion: One dominant conformation of the monohydrate of BC27 with OH_b signal at 3492 cm^{-1}, no need to invoke a resonance or second isomer at the present S/N ratio.

3.7 BC29+H_2O

BC29 was obtained from Sigma Aldrich (99%, Lot#SHBL6740), degassed and measured at 0.2 hPa partial pressure with slightly different amounts of H_2O (explicitly added + desorbed from the walls) in 750 hPa He, co-adding # gas pulses.

identifier	# pulses	p(BC29) hPa	p(H_2O) hPa	p(He) hPa	note
20210721-abcde	800	0.2	0.2	750	see figure 8, dark blue
20210722-abcde	700	0.2	0.25	750	see figure 8, blue

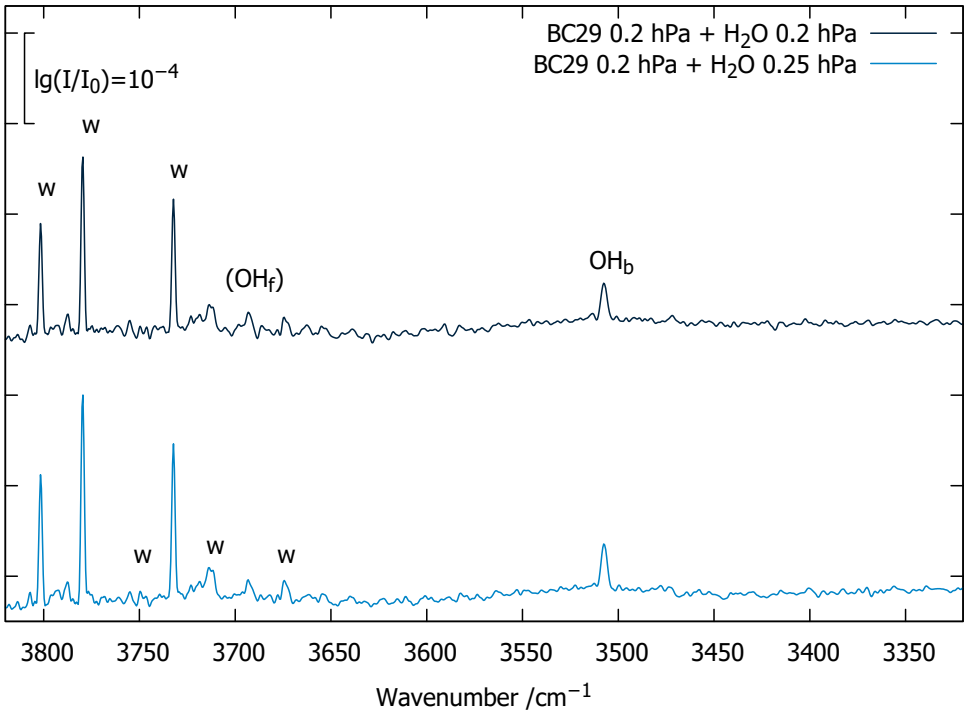

Figure 8: Jet cooled FTIR spectra of BC29 with H_2O at two slightly different concentrations (shades of blue). The mixed heterodimer is labeled OH_b.

The measurements show only one signal for the heterodimer of BC29+H_2O at 3507 cm^{-1} with a FWHM of about 4 cm^{-1} and the assignment is straightforward (see Fig. 8).

Exploratory quantum chemical calculations on B3LYP-D3(BJ)/def2-TZVP level predict only one stable heterodimer structure, consistent with the observations and with previous structural spectroscopy[16].

Conclusion: One dominant conformation of the monohydrate of BC29 with OH_b signal at 3507 cm^{-1}, no need to invoke a resonance or second isomer at the present S/N ratio.

3.8 BC30+H_2O

For the Raman spectra, BC30 was obtained from Sigma Aldrich (98%, S-form, 97% enantiopure, Lot#STBJ1541) and measured at different ratios with H_2O or $H_2{}^{18}O$, controlled by mass flow controllers, in 700 hPa He, co-adding recordings of a total duration of t_{tot} at a nozzle distance of 1 mm. The partial pressures are roughly estimated based on saturated vapor pressures and mass flow controller settings. The signals marked 'impurity' are largely due to sample impurities, as control measurements with fresh sample show (see Fig. 2 in the main article). They do not shift with ^{18}O substitution and therefore are not due to hydrate clusters.

identifier Raman	t_{tot} s	p(BC30) hPa	p(H_2O) hPa	p(He) hPa	note
20211027-a	6000	0.5	1	700	^{16}O, see figure 9, blue
20211215-a	6000	0.5	1	700	^{18}O, see figure 9, green

For the IR spectra, BC30 was obtained from Sigma Aldrich (98%, S-form, Lot#STBJ1541), degassed and measured at different partial pressures with different amounts of H_2O (explicitly added + desorbed from the walls) or $H_2{}^{18}O$ (slowly exchanging with water from the walls) in 750 hPa He, co-adding # gas pulses.

identifier IR	# pulses	p(BC30) hPa	p(H_2O) hPa	p(He) hPa	note
20210811-abcdef+0809-abcdef	600	0.1	0.2	750	^{18}O, see figure 9, dark green
20210810-abcdefg	800	0.1	0.2	750	^{16}O, see figure 9, dark blue

The monohydrate of BC30 is a special case, because the organic molecule already contains an OH group and the water OH_b stretching vibration couples with the solute OH stretching vibration. This renders Raman jet spectroscopy important, because the relative intensity pattern may vary from that of the IR spectrum. In the present case, the less downshifted transition at 3524 cm^{-1} is more IR-active (out-of-phase stretching induces more dipole change) and the further downshifted transition at 3474 cm^{-1} is more Raman-active (in-phase stretching induces more polarizability change), Furthermore, ^{18}O substitution in the water molecule reveals the dominant water character of the IR-active OH stretching mode (8 cm^{-1} isotope downshift - however, overlap with a BC30 cluster signal increases the band position uncertainty), but the water character of the Raman-active OH stretching mode is far from negligible (5 cm^{-1} isotope downshift). This could be challenging for models which focus only on a single OH stretching fundamental with water OH_b character.

Exploratory harmonic quantum chemical calculations on B3LYP-D3(BJ)/def2-TZVP level predict one dominant inserted 1:1 complex isomer and thus one signal for the BC30+H_2O complex, consistent with the observations upon BC30 and H_2O variation (see Fig. 9). In this case, it is essential that the insertion topology of the complex in a jet expansion has been unambiguously

identified before[9], because the insertion process could be kinetically hindered[35] and thus lead to the stabilization of a secondary isomer.

Conclusion: The global minimum conformation of the BC30 monohydrate has an OH_b-dominated signal at 3524 cm^{-1} (OH_{b1}) and a signal with less OH_b (and more BC30 OH) character at 3474 cm^{-1} (OH_{b2}). The presence of a resonance is difficult to judge due to the congestion with BC30 homocluster signals[36,37] (in particular in the OH_{b2} region). Further experiments are planned to disentangle these.

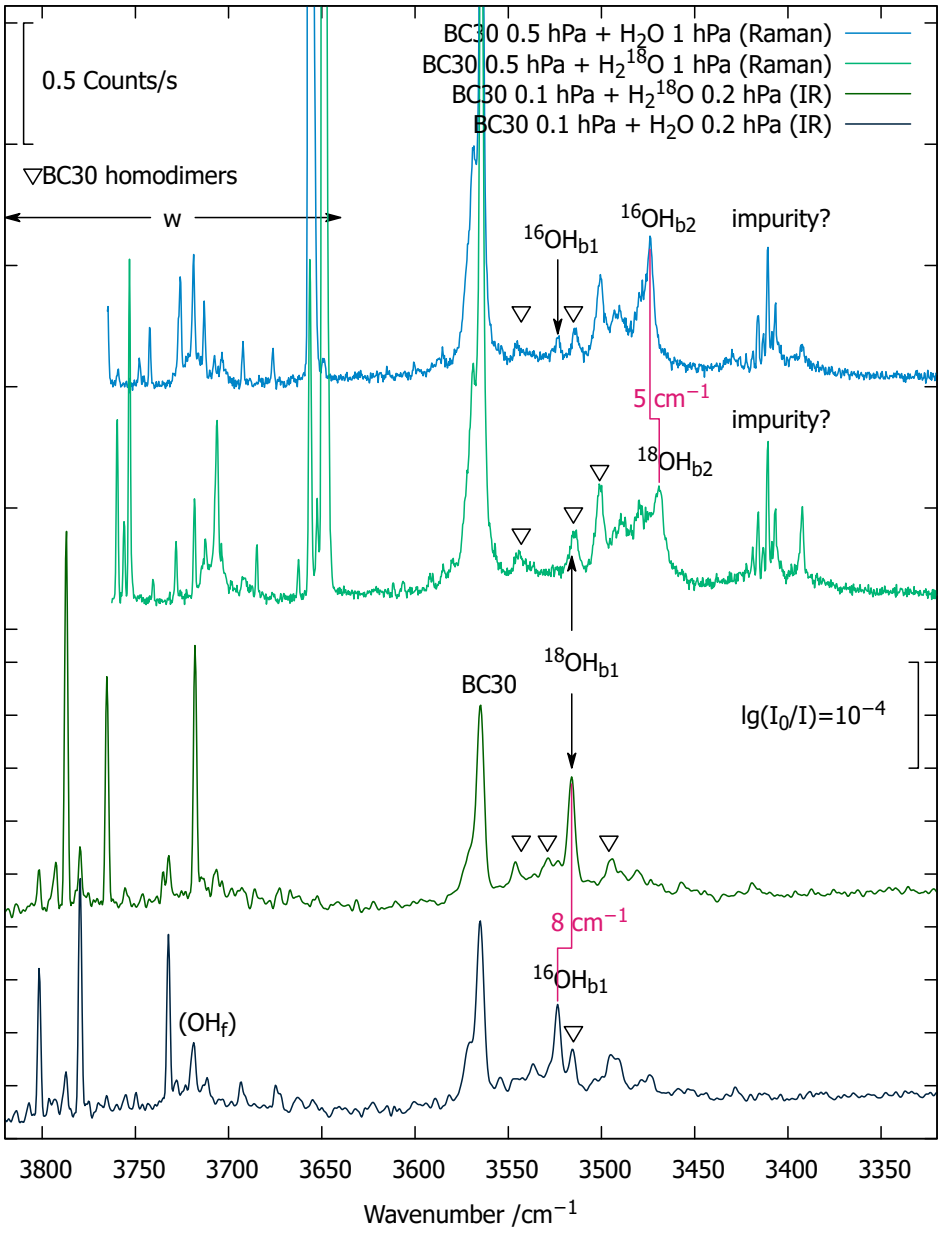

Figure 9: Jet cooled Raman (lighter colors) spectra of BC30 with H_2O (blue) and $H_2{}^{18}O$ (green) and FTIR spectra (darker tones) of BC30 with H_2O (dark blue) and $H_2{}^{18}O$ (dark green). The heterodimer bands of donor water are labeled as OH_{b1} for the dominant component and OH_{b2} for the BC30-centered OH vibration which carries some water stretching character, as judged by the isotope shift. The signal marked (OH_f) cannot be located reliably.

3.9 BC36+H_2O

BC36 was obtained from Santa Cruz Biotechnology (99% purity; enantiopurity >98%, Lot#2520) and placed at 363 K in an oven prior to the expansion. A flow of He with regular H_2O or $H_2{}^{18}O$ (Sigma Aldrich, 97%, Lot#MBBC9003) picked up the BC36 vapor and was expanded at 1500 hPa through a 200 μm pulsed nozzle (General Valve - Parker). Mass-resolved S_0-S_1 spectra were obtained using one-color resonance-enhanced two-photon ionization (RE2PI) spectroscopy, which allowed recording the vibrational spectra using the IR-UV double resonance method[38,39].

The UV laser beam (0.02 cm^{-1} resolution) was slightly focused (1 m focal length) in the interaction region of a linear time-of-flight (TOF) mass spectrometer. A counter-propagating IR beam (3 cm^{-1} resolution) was triggered 80 ns before the UV pulse and mildly focused (50 cm focal length) in the interaction region of the TOF. The IR spectra were recorded with an active baseline scheme, by measuring the difference in ion signal produced by successive UV laser pulses (one without and one with the IR laser pulse)[20]. Due to extensive fragmentation in the ion, the S_0-S_1 spectrum of the hydrates were recorded at the mass of the monomer. The absorption of the monohydrate is shifted up in energy by 68 cm^{-1} relative to the monomer and is identical for the two isotopomers.

Two depletion spectra are shown in Fig. 10. The upper trace involves regular water, the lower ^{18}O labeled water in the co-expansion. In each case, 4 peaks are observed. The highest wavenumber peak (3722 cm^{-1} for ^{16}O, 3707 cm^{-1} for ^{18}O) clearly corresponds to the free OH stretch and features an isotope shift of the expected magnitude. The other three signals correspond to hydrogen-bonded OH groups. Two of them do not change with isotope substitution (3542 and 3480 cm^{-1}) and thus correspond to the OH stretching fundamentals in the BC36 fragment. The third one (3597 cm^{-1}, with its maximum possibly shifted down slightly for ^{16}O, see below; 3589 cm^{-1} for ^{18}O) shows at least a 8 cm^{-1} isotope shift and corresponds to the water OH_b stretch which is of interest in this challenge. The deformation of the base line on each side of the 3597 cm^{-1} band is due to absorption by the monomer detected by non-resonant ionization[40]. The FWHM of the depletion signals (about 10 cm^{-1} and more for the strongly shifted bands) is a combination of laser bandwidth, rovibrational structure, vibrational energy redistribution and probably saturation.

BC36 was previously studied in CCl_4 solution[11] and found to exhibit two sharp OH stretching fundamentals (3549 and 3586 cm^{-1}), as expected. A weak signal at 3623 cm^{-1} was attributed to a secondary BC36 monomer conformation. The less shifted OH transition involves an OH-π interaction and the water is believed to insert into that contact. There is no known previous study of its monohydrate.

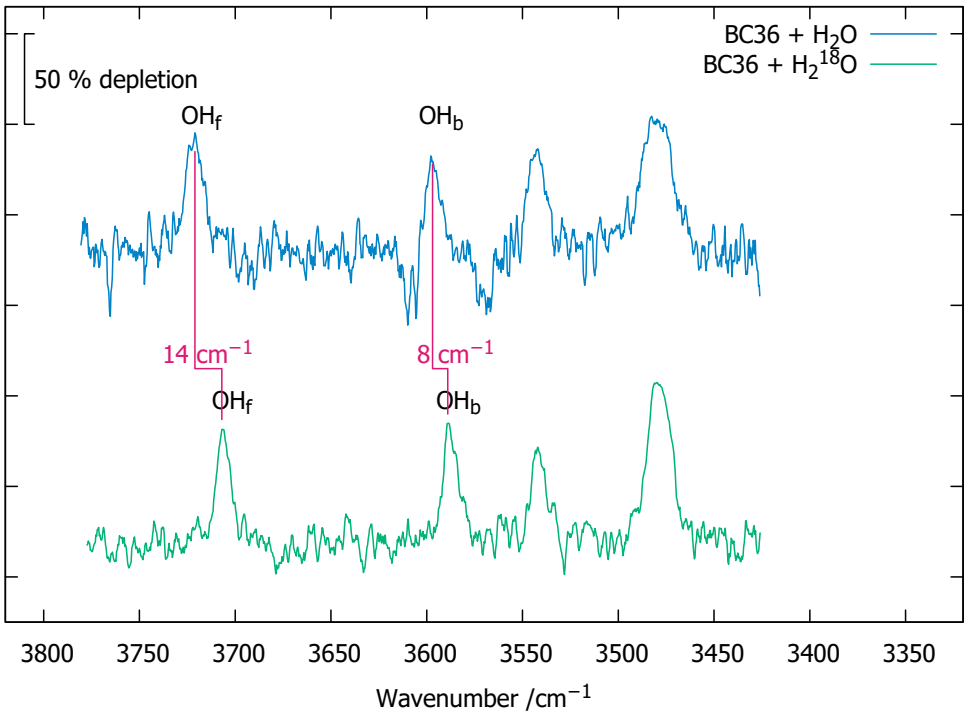

Figure 10: IR depletion spectra with mass detection for BC36 + H_2O and BC36 + $H_2^{18}O$ after 5-point smoothing, also indicating the isotope substitution wavenumber shifts which reveal the localized water vibrations.

Conclusion: One conformation of the monohydrate of BC36 with its water OH_b stretching fundamental at 3597 cm^{-1} or slightly higher and a 8 cm^{-1} ^{18}O isotope substitution downshift. No evidence for a second isomer or any vibrational resonance which would generate extra signals.

3.10 BC38+H_2O

The weak hydrogen bond of the water molecule in the monohydrate of BC38 to the F atom is very difficult to detect by IR spectroscopy, because it correlates with the low activity water symmetric stretching mode. Therefore, our study focuses on the Raman spectrum. For the Raman spectra, BC38 was obtained from abcr (99%, Lot#100918) and measured at different ratios with H_2O, controlled by mass flow controllers and roughly estimated based on vapor pressures, in 700 hPa He, co-adding recordings of a total duration of t_{tot} at a nozzle distance of 1 mm.

identifier Raman	t_{tot} s	p(BC38) hPa	p(H_2O) hPa	p(He) hPa	note
20210907_a	4800	1	1	700	see figure 11, light blue
20210908_a	5760	1	2	700	see figure 11, dark blue
20210907_c	4800	0	2	700	see figure 11, grey

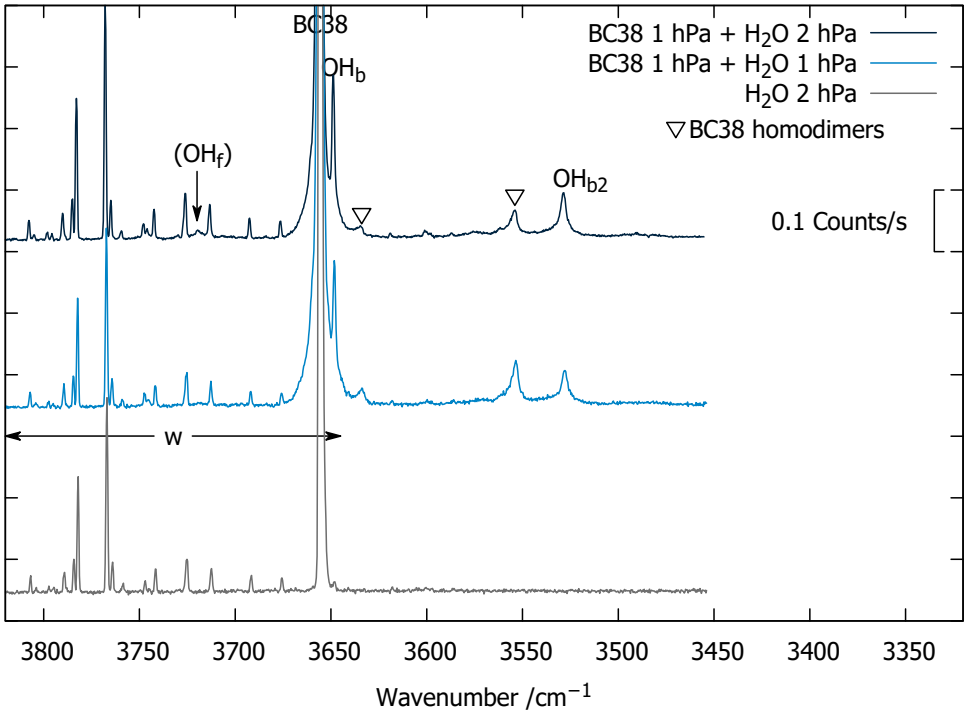

Figure 11: Jet cooled Raman spectra of H_2O with (blue) and without (grey) BC38. The heterodimer stretching band of the donor water is labeled as OH_b, the alcohol-localized vibration with OH_{b2}. The signal marked (OH_f) cannot be located reliably.

The free OH stretching vibration OH_f is located near 3719 cm^{-1}, embedded in water monomer transitions. The OH_b signal consists of a very prominent and sharp shoulder to the combined water monomer symmetric stretching band center and BC38 monomer OH stretching transition (both at 3657 cm^{-1}) at 3649 cm^{-1} (FWHM 2 cm^{-1}). To make sure that it does not overlap with a water monomer rovibrational line, a spectrum without BC38 addition is also shown. In

hindsight, this fundamental can also be spotted in the published IR jet spectrum at the highest cluster concentration reported[18], as a faint shoulder of the BC38 monomer signal. The alcoholic OH stretching fundamental is further downshifted at 3529 cm^{-1} (FWHM 4 cm^{-1}), in agreement with previous IR evidence[18].

Exploratory harmonic quantum chemical calculations on B3LYP-D3(BJ)/def2-TZVP level predict one dominant inserted 1:1 complex isomer and thus one signal for the BC38+H_2O complex, qualitatively consistent with the observations upon BC38 and H_2O variation (see Fig. 9) and with the structural evidence from microwave spectroscopy[19].

Conclusion: The global minimum conformation of the BC38 monohydrate has an OH_b signal at 3649 cm^{-1}, very weakly downshifted from the corresponding water monomer vibration.

4 Reinvestigation of the training set member aniline monohydrate by FTIR spectroscopy

Aniline (ANL) was obtained from Sigma Aldrich (for synthesis, Lot#S6047356213), degassed and measured at different partial pressures with different amounts of H_2O (explicitly added + desorbed from the walls) in 750 hPa He, co-adding # gas pulses.

identifier	# pulses	p(ANL) hPa	p(H_2O) hPa	p(He) hPa	note
20220502-abcd	1000	0.2	0.4	750	see figure 12, green
20220429-abcd	1000	0.2	<0.1	750	see figure 12, black
20220421-abcde+ 20220422-abcde	1900	0.1	0.4	750	see figure 12, blue
20220425-abcde+ 20220426-abcde	1800	0.1	<0.1	750	see figure 12, dark blue

The measurements show two strong NH stretching signals from ANL and only one strong signal for the heterodimer of ANL+H_2O at 3525 cm^{-1} with a FWHM of about XX cm^{-1}. Its assignment is straightforward (see Fig. 12). The band position agrees with a previous size-selected study[41] within the spectral resolution (3524 cm^{-1}). A satellite band at 3547 cm^{-1} observed before[41] is very weak in the linear spectra shown in Fig. 12 (hardly above the noise, less than 10% of the OH_b intensity) and can be ruled out as a significant resonance partner.

Conclusion: One dominant conformation of the monohydrate of ANL with OH_b signal at 3525 cm^{-1}, no need to invoke a resonance or second isomer at the present S/N ratio.

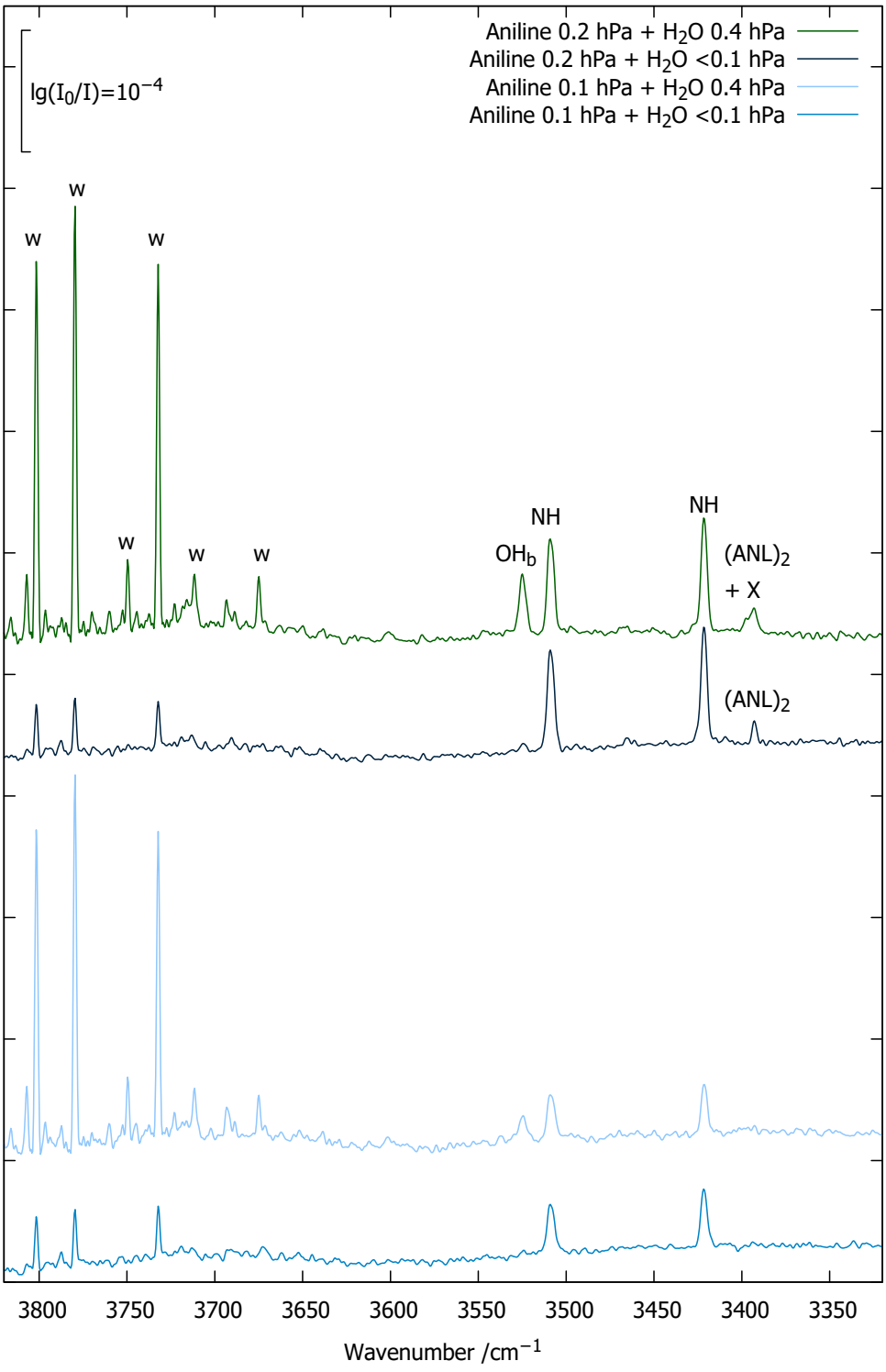

Figure 12: Jet cooled FTIR spectra of ANL with H_2O. The signal marked with OH_b scales with the water and ANL concentrations like a 1:1 complex. The ANL dimer signal which emerges at higher concentration is superimposed by signal from a complex with H_2O (X).

5 Conclusions

These experimental data on the 10 members of the HyDRA test set were made publically available shortly after the submission deadline for theory predictions and without knowledge of the latter[42]. Only typographical corrections, updated formulations, further references, and an analysis of the aniline monohydrate were added since then. The hydrogen bond donating water stretching fundamentals OH_b of the test set are found to spread over $195\,cm^{-1}$, slightly more than the training set[1,2]. The observed bands range from tiny to significant downshifts relative to the water monomer symmetric stretch at $3657\,cm^{-1}$, without leading to excessive anharmonic coupling patterns which would qualitatively invalidate scaled harmonic theory approaches. Still, anharmonicity corrections, once affordable, are expected to be significant and non-uniform. The previous assignment of the training system aniline monohydrate was confirmed by linear absorption spectroscopy, with a best band center estimate of $3525\,cm^{-1}$ and no evidence for a significant resonance interaction.

Author contributions

T.L.F.: Data curation, Formal analysis, Investigation, Visualization, Writing - review & editing; M.B.: Data curation, Investigation, Visualization, Writing - review & editing; S.M.S.: Investigation, Visualization, Writing - review & editing; J.D.: Investigation, Visualization, Writing - review & editing; V.L.: Investigation, Visualization, Writing - review & editing; A.Z.: Investigation, Methodology, Validation, Writing - review & editing ; M.A.S.: Conceptualization, Formal Analysis, Funding acquisition, Investigation, Methodology, Project administration, Resources, Supervision, Validation, Writing – original draft, Writing – review & editing

ORCID

T.L.F. 0000-0003-2050-3628; M.B. 0000-0002-5883-3801; S.M.S. 0000-0002-3827-0642; V.L. 0000-0001-5955-4372; A.Z. 0000-0001-5540-0667; M.A.S. 0000-0001-8841-7705;

Acknowledgements

This work was funded by the Deutsche Forschungsgemeinschaft (DFG, German Research Foundation) - 389479699/GRK2455. The FTIR and Raman experiments would not have been possible without the superb support of the Goettingen mechanics, glass and electronics workshops. We thank Maxim Gawrilow and Beppo Hartwig for help and discussions.

References

[1] Fischer, T.; Bödecker, M.; Zehnacker, A.; Mata, R.; Suhm, M. Setting up the HyDRA blind challenge for the microhydration of organic molecules. *ChemRxiv* **2021**, DOI:10.26434/chemrxiv–2021–w8v42.

[2] Fischer, T. L.; Bödecker, M.; Zehnacker-Rentien, A.; Mata, R. A.; Suhm, M. A. Setting up the HyDRA blind challenge for the microhydration of organic molecules. *Phys. Chem. Chem. Phys.* **2022**, *24*, 11442–11454.

[3] Burevschi, E.; Peña, I.; Sanz, M. E. Geminal diol formation from the interaction of a ketone with water in the gas phase: Structure and reactivity of cyclooctanone-(H_2O) 1, 2 clusters. *The Journal of Physical Chemistry Letters* **2021**, *12*, 12419–12425.

[4] Burevschi, E.; Peña, I.; Sanz, M. E. Medium-sized rings: Conformational preferences in cyclooctanone driven by transannular repulsive interactions. *Physical Chemistry Chemical Physics* **2019**, *21*, 4331–4338.

[5] Vrolix, E.; Goethals, M.; Zeegers-Huyskens, T. Infrared study of hydrogen bond complexes involving 1, 3-dimethyl, 2-imidazolidinone and hydroxylic derivatives. *Spectroscopy Letters* **1993**, *26*, 497–507.

[6] Vigorito, A.; Paoloni, L.; Calabrese, C.; Evangelisti, L.; Favero, L. B.; Melandri, S.; Maris, A. Structure and dynamics of cyclic amides: The rotational spectrum of 1, 3-dimethyl-2-imidazolidinone. *Journal of Molecular Spectroscopy* **2017**, *342*, 38–44.

[7] Nelander, B. A matrix isolation study of the water-formaldehyde complex. The far-infrared region. *Chemical Physics* **1992**, *159*, 281–287.

[8] Lovas, F. J.; Lugez, C. L. The microwave spectrum and structure of CH_2O–H_2O. *Journal of Molecular Spectroscopy* **1996**, *179*, 320–323.

[9] Thomas, J.; Sukhorukov, O.; Jäger, W.; Xu, Y. Direct spectroscopic detection of the orientation of free OH groups in methyl lactate–(water) 1, 2 clusters: Hydration of a chiral hydroxy ester. *Angewandte Chemie International Edition* **2014**, *53*, 1156–1159.

[10] Katsyuba, S. A.; Spicher, S.; Gerasimova, T. P.; Grimme, S. Revisiting conformations of methyl lactate in water and methanol. *The Journal of Chemical Physics* **2021**, *155*, 024507.

[11] Galantay, E. 1-phenylcyclohexane-1,2-diols and their geometry. *Tetrahedron* **1963**, *19*, 319–321.

[12] Nieto, P.; Letzner, M.; Endres, T.; Schwaab, G.; Havenith, M. IR spectroscopy of pyridine–water structures in helium nanodroplets. *Physical Chemistry Chemical Physics* **2014**, *16*, 8384–8391.

[13] Mackenzie, R. B.; Dewberry, C. T.; Cornelius, R. D.; Smith, C.; Leopold, K. R. Multidimensional large amplitude dynamics in the pyridine–water complex. *The Journal of Physical Chemistry A* **2017**, *121*, 855–860.

[14] Melnik, D. G.; Gopalakrishnan, S.; Miller, T. A.; De Lucia, F. C. The absorption spectroscopy of the lowest pseudorotational states of tetrahydrofuran. *The Journal of Chemical Physics* **2003**, *118*, 3589–3599.

[15] Sahu, P. K.; Lee, S.-L. Hydrogen-bond interaction in 1:1 complexes of tetrahydrofuran with water, hydrogen fluoride, and ammonia: A theoretical study. *The Journal of Chemical Physics* **2005**, *123*, 044308.

[16] Sanz, M. E.; López, J. C.; Alonso, J. L.; Maris, A.; Favero, P. G.; Caminati, W. Conformation and stability of adducts of sulfurated cyclic compounds with water: Rotational spectrum of tetrahydrothiophene–water. *The Journal of Physical Chemistry A* **1999**, *103*, 5285–5290.

[17] Lei, J.; Alessandrini, S.; Chen, J.; Zheng, Y.; Spada, L.; Gou, Q.; Puzzarini, C.; Barone, V. Rotational spectroscopy meets quantum chemistry for analyzing substituent effects on non-covalent interactions: The case of the trifluoroacetophenone-water complex. *Molecules* **2020**, *25*, 4899.

[18] Heger, M.; Scharge, T.; Suhm, M. A. From hydrogen bond donor to acceptor: The effect of ethanol fluorination on the first solvating water molecule. *Physical Chemistry Chemical Physics* **2013**, *15*, 16065–16073.

[19] Thomas, J.; Xu, Y. Structure and tunneling dynamics in a model system of peptide cosolvents: Rotational spectroscopy of the 2,2,2-trifluoroethanol$\cdots$water complex. *The Journal of Chemical Physics* **2014**, *140*, 06B616_1.

[20] Sen, A.; Bouchet, A.; Lepère, V.; Le Barbu-Debus, K.; Scuderi, D.; Piuzzi, F.; Zehnacker-Rentien, A. Conformational analysis of quinine and its pseudo enantiomer quinidine: A combined jet-cooled spectroscopy and vibrational circular dichroism study. *The Journal of Physical Chemistry A* **2012**, *116*, 8334–8344.

[21] Hartwig, B.; Suhm, M. A. Subtle hydrogen bonds: benchmarking with OH stretching fundamentals of vicinal diols in the gas phase. *Physical Chemistry Chemical Physics* **2021**, *23*, 21623–21640.

[22] Gottschalk, H. C.; Fischer, T. L.; Meyer, V.; Hildebrandt, R.; Schmitt, U.; Suhm, M. A. A sustainable slit jet FTIR spectrometer for hydrate complexes and beyond. *Instruments* **2021**, *5*, 12.

[23] Nelander, B. Infrared spectrum of the water formaldehyde complex in solid argon and solid nitrogen. *The Journal of Chemical Physics* **1980**, *72*, 77–84.

[24] Ha, T. K.; Makarewicz, J.; Bauder, A. Ab initio study of the water-formaldehyde complex. *The Journal of Physical Chemistry* **1993**, *97*, 11415–11419.

[25] Dimitrova, Y.; Peyerimhoff, S. D. Theoretical study of hydrogen-bonded formaldehyde-water complexes. *The Journal of Physical Chemistry* **1993**, *97*, 12731–12736.

[26] Ramelot, T. A.; Hu, C.-H.; Fowler, J. E.; DeLeeuw, B. J.; Schaefer, H. F. Carbonyl–water hydrogen bonding: The H_2CO–H_2O prototype. *The Journal of Chemical Physics* **1994**, *100*, 4347–4354.

[27] Millen, D. J.; Mines, G. W. Hydrogen bonding in the gas phase. Part 5.—Infrared spectroscopic investigation of O–H$\cdots$N complexes formed by water: Ammonia monohydrate and amine and pyridine monohydrates. *Journal of the Chemical Society, Faraday Transactions 2: Molecular and Chemical Physics* **1977**, *73*, 369–377.

[28] Choi, M. Y.; Miller, R. E. Infrared laser spectroscopy of imidazole complexes in helium nanodroplets: Monomer, dimer, and binary water complexes. *The Journal of Physical Chemistry A* **2006**, *110*, 9344–9351.

[29] Zischang, J.; Lee, J. J.; Suhm, M. A. Communication: Where does the first water molecule go in imidazole? *The Journal of Chemical Physics* **2011**, *135*, 061102.

[30] Destexhe, A.; Smets, J.; Adamowicz, L.; Maes, G. Matrix isolation FT-IR studies and ab initio calculations of hydrogen-bonded complexes of molecules modeling cytosine or isocytosine tautomers. 1. Pyridine and pyrimidine complexes with water in argon matrixes. *J. Phys. Chem.* **1994**, *98*, 1506–1514.

[31] Feng, J.-Y.; Lee, Y.-P.; Witek, H. A.; Hsu, P.-J.; Kuo, J.-L.; Ebata, T. Structures of Pyridine–Water Clusters Studied with Infrared–Vacuum Ultraviolet Spectroscopy. *The Journal of Physical Chemistry A* **2021**, *125*, 7489–7501.

[32] Shultz, M. J.; Vu, T. H. Hydrogen bonding between water and tetrahydrofuran relevant to clathrate formation. *The Journal of Physical Chemistry B* **2015**, *119*, 9167–9172.

[33] Meyer, R.; López, J. C.; Alonso, J. L.; Melandri, S.; Favero, P. G.; Caminati, W. Pseudorotation pathway and equilibrium structure from the rotational spectrum of jet-cooled tetrahydrofuran. *The Journal of Chemical Physics* **1999**, *111*, 7871–7880.

[34] Fischer, T. L.; Wagner, T.; Gottschalk, H. C.; Nejad, A.; Suhm, M. A. A rather universal vibrational resonance in 1:1 hydrates of carbonyl compounds. *The Journal of Physical Chemistry Letters* **2021**, *12*, 138–144.

[35] Borho, N.; Suhm, M. A.; Le Barbu-Debus, K.; Zehnacker, A. Intra- vs. intermolecular hydrogen bonding: dimers of alpha-hydroxyesters with methanol. *Physical Chemistry Chemical Physics* **2006**, *8*, 4449–4460.

[36] Borho, N.; Suhm, M. A. Self-organization of lactates in the gas phase. *Organic & Biomolecular Chemistry* **2003**, *1*, 4351–4358.

[37] Zielke, P.; Suhm, M. A. Concerted proton motion in hydrogen-bonded trimers: A spontaneous Raman scattering perspective. *Physical Chemistry Chemical Physics* **2006**, *8*, 2826–2830.

[38] Pribble, R. N.; Zwier, T. S. Size-specific infrared spectra of benzene-$(H_2O)_n$ clusters (n= 1 through 7): Evidence for noncyclic $(H_2O)_n$ structures. *Science* **1994**, *265*, 75–79.

[39] Tanabe, S.; Ebata, T.; Fujii, M.; Mikami, N. OH stretching vibrations of phenol—$(H_2O)_n$ (n= 1–3) complexes observed by IR-UV double-resonance spectroscopy. *Chemical Physics Letters* **1993**, *215*, 347–352.

[40] Omi, T.; Shitomi, H.; Sekiya, N.; Takazawa, K.; Fujii, M. Nonresonant ionization detected IR spectroscopy for the vibrational study in a supersonic jet. *Chemical Physics Letters* **1996**, *252*, 287–293.

[41] León, I.; Arnáiz, P.; Usabiaga, I.; Fernández, J. Mass resolved IR spectroscopy of aniline–water aggregates. *Physical Chemistry Chemical Physics* **2016**, *18*, 27336–27341.

[42] Suhm, M. A.; Zehnacker-Rentien, A.; Lepère, V.; Dupont, J.; Schweer, S. M.; Bödecker, M.; Fischer, T. L. Experimental Supplement to the HyDRA blind challenge. 2022; `https://doi.org/10.25625/FLGZYE`.